Techniques and Performance of Intensity-Modulation Direct-Detection Analog Optical Links

Charles Cox III, *Senior Member, IEEE,* Edward Ackerman, *Member, IEEE,*
Roger Helkey, *Member, IEEE,* and Gary E. Betts, *Member, IEEE*

Abstract— We review state-of-the-art intensity-modulation direct-detection (IMDD) analog optical links, focusing on advances since 1990. We contrast direct and external modulation with respect to gain, noise figure (NF), and dynamic-range (DR) performance.

Index Terms— Electro-optic modulators, modeling, noise, nonlinearities, optical fiber communication, optical modulation/demodulation, optoelectronic devices, photodetectors, semiconductor lasers.

I. INTRODUCTION

FOR applications such as the distribution of cable-television signals, antenna remoting of cellular/personal-communication system (PCS) signals, and beam forming for phased-array radars, there has been significant progress in the design and performance of analog optical links. This review focuses on the developments in intensity-modulation direct-detection (IMDD) links that have been reported over the last six years. For a comprehensive overview of coherent detection links, the reader is referred to a recent review by Seeds [1].

As shown in Fig. 1, we define a link as consisting of all the hardware required to modulate the RF signal onto the optical carrier, the optical transmission medium, and the hardware required to recover the RF from the optical carrier. Also included in the link definition are any passive impedance-matching circuits used to match the modulation device and photodetector impedances to the RF source and load impedances, respectively. By limiting the discussion to amplifierless links, we more easily see the effects that device parameters have on the link parameters. The process of combining a link with amplifiers involves many tradeoffs which are beyond the scope of this paper.

The discussion here is further limited to the basic measures of link performance which affect a wide variety of applications: gain, noise figure (NF), and dynamic range (DR). Unless otherwise indicated, all the results reported below are for links operating at optical wavelengths of either 1.3 or 1.55 μm, which are the dominant ones in use because of the availability of optical fiber with low loss and near-zero dispersion at these wavelengths.

The organization of the material in this paper is as follows. The photodetection process is discussed first since this is common to all IMDD links. The two principal intensity-modulation techniques—direct and external modulation—are discussed next, along with their maximum modulation frequencies. Direct and external modulation-link performance is compared on the basis of the three main link figures of merit: gain, NF, and intermodulation-free DR.

II. PHOTODETECTORS

Virtually all photodetectors in use today are based on the p-i-n structure; consequently the emphasis will be on this type of detector in the discussion below. Long wavelength—i.e., 1.3 and 1.55 μm—avalanche photodiodes have been developed, but they have approximately an order of magnitude lower avalanche gain at the same excess noise factor than silicon avalanche photodiodes [2]. Photoconductors [3] and direct illumination of phototransistors [4] have also been investigated for their potential use as photodetectors.

As is evident from the summary of reported results shown in Fig. 2 (based on data in [5]–[15]), photodetectors are available with 3-dB bandwidths which are more than sufficient for most link applications. However, the highest bandwidths come at a penalty to the detector responsivity. As will be seen below, the square of this parameter is a term in the equation for link gain. At any optical wavelength λ, the ideal responsivity of any photodetector is simply the electron charge q divided by the photon energy hc/λ (where h is Planck's constant and c is the speed of light in a vacuum). At 1.3 μm this works out to about 1.05 A/W. Therefore, at low frequencies, where some commercially available 1.3-μm photodetectors have fiber-coupled responsivities of 0.9 A/W, this factor contributes only about 1.3 dB $(= 20\cdot\log[0.9/1.05])$ to the link RF-to-RF loss (as shown on the right-hand axis of Fig. 2), whereas at higher frequencies a typical photodetector responsivity of 0.1 A/W would contribute 20.4 dB to the link loss. The reason for this tradeoff is reasonably fundamental to the surface-illuminated configuration: to avoid bandwidth limiting effects, the photodetector volume is decreased; however, this small photodetector volume is less efficient at absorbing the light, thereby decreasing the responsivity as well.

Another photodetector tradeoff is between linearity and optical power. All IMDD links have a reason to operate at high optical power. For direct modulation, the maximum modulation frequency of diode lasers is proportional to the square root of optical power [16]. For external modulation,
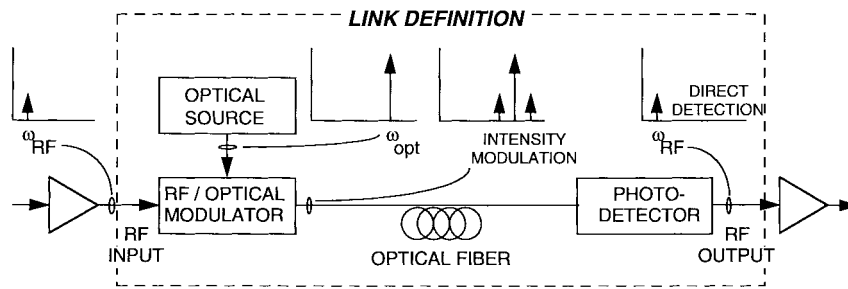
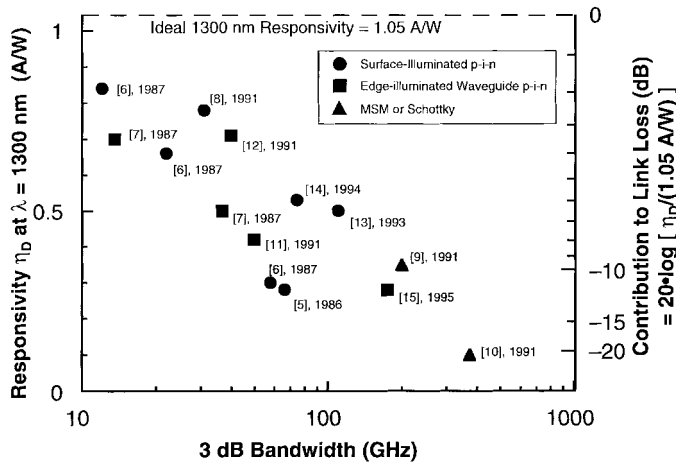Fig. 1. Definition of IMDD analog optical link.

Fig. 2. Responsivities and 3-dB bandwidths of state-of-the-art photodetectors, as reported in [5]–[15]. For cases where responsivities were reported at other wavelengths, equivalent 1300-nm responsivities were calculated from reported external quantum efficiencies.

Fig. 3. Summary of direct and external modulation-link gains reported in the literature [20]–[25], [30]–[36] across various frequency bands.

the link gain is proportional to the square of optical power, as will be discussed further on. Unfortunately, photodetector nonlinearities begin to dominate over modulation-device nonlinearities at high optical power densities. Recent results suggest that photodiode nonlinearities can be reduced by increasing the bias, since at high detector currents the series resistance and/or space-charge effects reduce the fraction of the bias voltage which actually appears as a field across the junction at higher optical powers [17].

This linearity/power-density problem can be largely avoided at low frequencies by using a sufficiently large photodetector area to keep the optical power-density low. Davis *et al.* [18] have recently achieved a combination of bandwidth (295 MHz) and maximum photocurrent (150 mA). At higher frequencies, the photodetector area must be decreased so the corresponding capacitance does not limit the bandwidth, which conflicts with maximizing the area to keep the power density low.

The linearity/power-density conflict can be significantly reduced by changing the photodetector illumination geometry from perpendicular to the junction (as in a surface-illuminated photodetector), to parallel to the junction (as in an edge-illuminated photodetector). The increase in maximum power density and corresponding saturation power was studied by Lin *et al.* [19]. Further improvement over the edge-illuminated photodetector should be attainable from the velocity-matched distributed photodetector geometry, wherein an RF transmis-
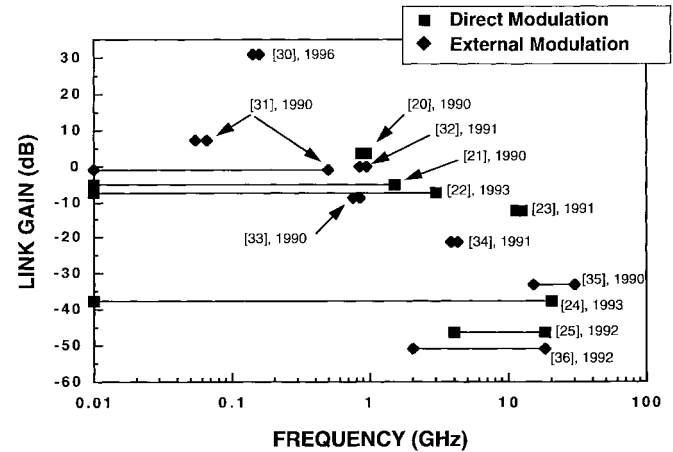
sion line sums the outputs of discrete photodetectors which are located along an optical waveguide [19]. Detector currents of 56 mA have been experimentally demonstrated at 0.85 μm in a 49-GHz velocity-matched distributed photodetector. Currently, the typical maximum photocurrent of a commercial 50-GHz photodetector is about 1–2 mA.

In summary, at low frequencies, photodetectors are nearly ideal in terms of responsivity, power handling, and linearity. Bandwidths for almost any imaginable application have been demonstrated, but are of limited usefulness at present because of limited responsivity and optical power density. For a more comprehensive overview of the present state-of-the-art photodetectors, the reader is referred to the recent review by Yu [2].

III. INTENSITY-MODULATION METHODS FOR DIRECT DETECTION

A. Direct Modulation

Virtually all direct modulation IMDD links use diode lasers with one of two laser cavity designs: Fabry–Perot (FP) or distributed feedback (DFB). Some low performance links use light-emitting diodes. To date, vertical-cavity surface-emitting lasers (VCSEL's) have not had a significant impact on analog-link designs, at least partially because the majority of the efforts have been at 0.85 μm, where the VCSEL material and fabrication problems are more tractable but optical-fiber loss and chromatic dispersion are high.
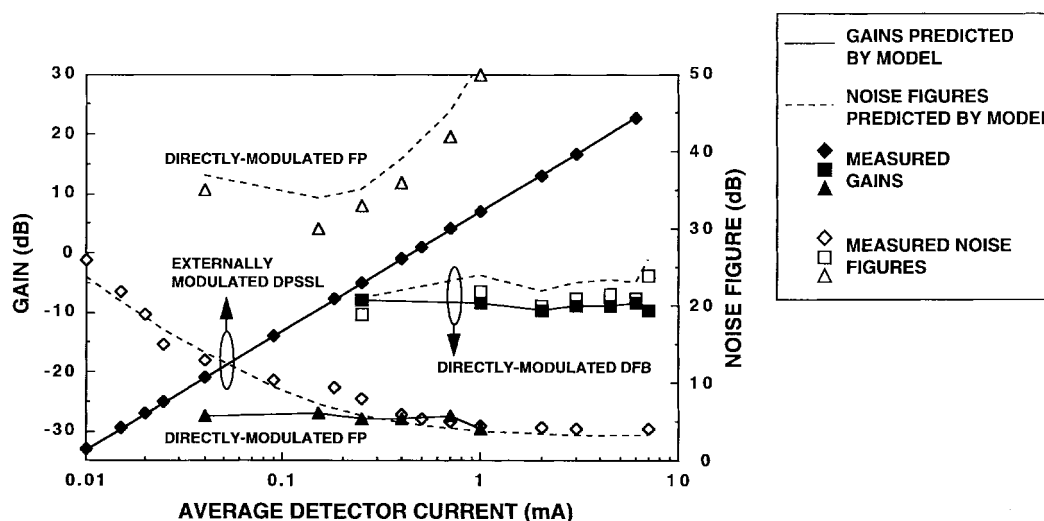
Fig. 4. Analytically determined (lines) and measured (points) gain and NF at several values of average detector current for links using the following three different combinations of optical source and modulator: 1) diode-pumped solid-state laser (DPSSL) externally modulated by a LiNbO$_3$ MZI modulator; 2) directly modulated DFB laser; and 3) directly modulated FP laser.

Some recently reported [20]–[25] IMDD direct modulation-link gains[1] are plotted versus frequency in Fig. 3. Note that except for one result [20], all the direct modulation-link gains are less than 0 dB. This is a simple consequence of conservation of energy which limits the product of laser-diode slope efficiency and photodetector slope efficiencies to be less than one. As will be discussed further on, although the direct modulation-link gain is independent of average optical power, the gain is proportional to the square of the laser's fiber-coupled slope efficiency. Coupling the highly divergent diode-laser beam into the low-divergence mode of a fiber is relatively inefficient, making the single-mode fiber-coupled slope efficiencies of commercially available devices typically 10%–50% of the diode-chip slope efficiency. The fiber-coupled slope efficiencies of presently available diode lasers range from 0.1 to 0.32 W/A [26]. Using the highest value of slope efficiency and assuming all the other link losses are negligible, the link loss would be −9.5 dB.

An obvious way to improve the gain of directly modulated links would be to use a type of semiconductor laser with higher laser-slope efficiency, such as the gain-lever laser [27]. However, initial attempts to achieve high link gain using this laser have been unsuccessful. Further, the substantial nonlinearity of this laser's p versus i curve (as shown in [27]) suggests that its IM-free DR will be unacceptable for the majority of analog-link applications.

Another way to improve link gain is to accept reduced bandwidth for increased link gain. Many antenna remoting and some CATV applications can use this approach. One way to make this tradeoff is to replace the conventional resistive (i.e., lossy) impedance match with an ideally lossless reactive impedance-matching circuit. Since the real part of the laser impedance is typically less than the 50-Ω source impedance and the photodetector impedance is typically greater than the 50-Ω load impedance, it is possible to make the ratio

of photodetector to modulation-device resistances R_D/R_{MD} greater than the product of the square of the slope efficiencies, thereby using the gains from impedance matching to completely overcome the electro-optical slope efficiency losses. This was demonstrated by Ackerman *et al.* [20], whose direct modulation-link result is the one in Fig. 4 with a gain greater than 0 dB.

Another important conclusion that can be drawn from the data shown in Fig. 3 is that the maximum bandwidth of direct modulation links is roughly 20 GHz. The maximum broad-band frequency response that has been *demonstrated* for a diode laser is 33 GHz. This high 3-dB bandwidth (defined with respect to the low-frequency response) was obtained by damping the laser's 22-GHz relaxation oscillation so that the gain rolled off very slowly above this frequency [28]. However, at frequencies near the relaxation oscillation frequency, a laser's noise and distortion increases, which in turn degrades the NF and DR around this frequency. Therefore, the maximum *usable* bandwidth for direct modulation analog links can be considerably less than the maximum 3-dB bandwidth.

It has been shown that the relaxation resonance frequency is proportional to the square root of the average optical power [16]. To achieve the record 33-GHz response required operating the laser at a bias current 10–12 times greater than the minimum current for lasing. To achieve further bandwidth increases via simple increases in the optical power will be difficult because of the laser heating due to the higher bias current. Different diode-laser active-layer architectures, such as the multiple quantum-well structure employed in the 33-GHz laser in [28], have been analytically determined to be capable of achieving much higher bandwidths, but to date the experimental demonstrations have not borne out the theory.

For applications that only require a very narrow passband, the present bandwidth limit of semiconductor lasers can be circumvented by exploiting the enhanced modulation response

---

[1] The term gain will be used here in the general sense where negative gain denote loss.

at frequencies that are at or near the laser-cavity round-trip time. Lau [29] has demonstrated modulation at 40 GHz, albeit with a 3-dB passband width of 200 MHz.

B. External Modulation

At present, the external modulator that is in commercial use and against which all newcomers are judged is the Mach–Zehnder interferometric (MZI) modulator fabricated in the inorganic material lithium niobate. When operated at wavelengths longer than approximately 1 μm, these modulators are capable of handling at least 400 mW of CW optical power [30] with only negligible degradation due to photo-refractive or optical-damage effects. Low-loss waveguides, fabricated via either titanium in-diffusion or proton exchange, together with efficient waveguide-to-fiber coupling have resulted in typical fiber-to-fiber optical losses of 4 dB, with losses as low as 2.5 dB achieved in the laboratory. Lumped-electrode modulators with a V_π of 0.65 V have been demonstrated [30] at 150 MHz. Higher frequency lumped-element modulators have a response that falls off roughly as the square of frequency. This trend can be seen from the recent IMDD external modulation-link results [30]–[36] plotted alongside the direct modulation-link results in Fig. 3.

At sufficiently high frequencies—specifically, a few gigahertz in lithium niobate—the modulation voltage cannot be approximated as constant during an optical transit time through the modulator. For this case, the most efficient modulation is achieved by using traveling-wave RF electrodes, whose propagation velocity matches the optical waveguide propagation velocity. In lithium niobate this velocity-match condition turns out to be difficult to achieve while simultaneously achieving a 50-Ω traveling-wave electrode impedance. The best velocity match has been reported by Noguchi *et al.* [37], who demonstrated a modulator with a 3-dB electrical bandwidth of 70 GHz and a V_π of 5 V.

Modulation at even higher frequencies is possible in lithium niobate, provided one can solve the problem of coupling the modulation signal onto the electrodes. An elegant solution to this problem has been proposed and demonstrated by Bridges *et al.*, [38], who separated the electrodes into segments with a dipole antenna element feeding each one. A velocity match is achieved by judicious angling of the modulator substrate relative to the end of the millimeter-waveguide which feeds the dipole antennas. Using this technique, Bridges *et al.* demonstrated bandpass modulation around 94 GHz.

Although a lithium–niobate MZI is the industry standard, it is not without its drawbacks. Its transfer function yields insufficient linearity for CATV distribution and other more demanding applications. Lithium niobate is difficult to work with and virtually impossible to integrate with electronic semiconductors. Also, the cost of a lithium–niobate MZI is high for what is basically a simple device.

One alternative, which avoids both the MZI structure and the lithium–niobate material, is the electro-absorption (EA) modulator. Initially, this type of modulator was believed to be of limited utility because its transfer function, which is based on the semiconductor absorption-band edge's dependency on the electric field, was more nonlinear than an MZI's. However, as demonstrated by Welstand *et al.* [39], by balancing the Franz–Keldysh effect with the quantum-confined Stark effect, it is possible to fabricate an EA modulator with greater linearity than that of a standard MZI. EA modulators do require wavelength control of the CW source on the order of 40 nm, which MZI's do not. Also, to our knowledge the greatest optical power that has been launched into an EA modulator to date is 34 mW [40], versus 400 mW for MZI's [30].

Another alternative to the standard lithium–niobate MZI is to stay with the MZI configuration—which, as will be shown below, can be *linearized* in a number of ways to increase its DR—but fabricate it in a different material. Semiconductors have been used as alternative materials for MZI's, resulting in modulation efficiencies (as measured by the switching voltage V_π) on par with lithium–niobate MZI's, albeit typically with greater than 10 dB of fiber-coupled insertion loss—mostly due to optical-mode mismatch between the fiber and semiconductor waveguides. Walker [41] has reported MZI's fabricated in GaAs, which in principal could be monolithically integrated with other electronics such as driver amplifiers. Nonlinear optical polymers have also been used to fabricate MZI's with frequency responses as high as 60 GHz [42]. Polymers hold the potential of lower cost and perhaps greater bandwidth, but to date neither of these attributes has been realized in a commercial modulator.

Alternatively one could stay with lithium niobate but use a different modulator structure, such as a directional-coupler modulator (DCM), which enables a variety of linearization techniques for increasing a link's DR. However, it is difficult to achieve a high-sensitivity modulation response in DCM's; in MZI's, higher sensitivity can be obtained by simply lengthening the electrodes, whereas lengthening the DCM's electrodes means redesigning the coupling region as well. Conceptually, DCM's could be fabricated in materials other than LiNbO$_3$, but the authors are unaware of any such work to date.

IV. MEASURES OF IMDD-LINK PERFORMANCE

A. Link Gain

It has been shown [43] that the IMDD-link gain can be expressed as a function of the fiber-coupled modulation-device and photodetector slope efficiencies (S_{MD} and S_D, with dimensions of W/A and A/W, respectively) and impedances (R_{MD}, R_D), namely

$$g = S_{\mathrm{MD}}^2 S_D^2 \frac{R_D}{R_{\mathrm{MD}}}. \qquad (1)$$

Expressions for direct and external modulation-link gain are derived by substituting into (1) the appropriate values of the device slope efficiencies and resistances. In the case of a direct modulation-link, $R_{\mathrm{MD}} = R_{\mathrm{Las}}$, and S_{MD} is simply S_L, the fiber-coupled external differential quantum efficiency of the directly modulated semiconductor laser; therefore,

$$g_{\mathrm{Dir}} = S_L^2 S_D^2 \frac{R_D}{R_{\mathrm{Las}}}. \qquad (2)$$

In the case of an external modulation-link, $R_{\mathrm{MD}} = R_{\mathrm{Mod}}$ (the equivalent parallel resistance of the modulator), and S_{MD} is related to the fiber-to-fiber optical transmission efficiency of the external modulator t_{ff}, the CW input optical power to the modulator P_I, and the modulator half-wave or on–off switching voltage V_π, resulting in the following expression for gain:

$$g_{\mathrm{ext}} = \left(\frac{t_{\mathrm{ff}} P_I \pi}{2 V_\pi} \right)^2 S_D^2 R_{\mathrm{Mod}} R_D. \tag{3}$$

An important distinction between (2) and (3) is the dependence on average optical power: (2) for direct modulation is independent of optical power, whereas (3) for external modulation depends quadratically on optical power. This distinction in optical power dependency has been confirmed experimentally as shown by the direct and external link gain data shown in Fig. 4. The direct modulation gain is independent of optical power, at least until average power levels are reached where the laser's P versus I curve begins to saturate. In the case of the direct modulation links in Fig. 4, the gain is higher when a DFB rather than a FP laser is used, simply because the former had a higher slope efficiency than the latter.

As shown in Fig. 4, the external modulation-link gain increases as the square of CW optical power, even achieving net available RF power gain for optical powers above 30 mW for links at frequencies below approximately 1 GHz. That net gain resulting from what may initially appear to be a passive circuit can be a bit unsettling at first. One intuitive explanation for the net gain starts with the fact that the RF impedance of the modulator is independent of the optical power flowing through the modulator. Consequently, the RF power at the link input is independent of the average optical power. However, the RF power recovered at the photodetector output clearly depends on the average optical power. For example, in the extreme case where the laser power is zero, the RF output from the detector is also zero. Therefore, as the average optical power is increased, the RF input power remains constant, but the RF power from the photodetector increases. It turns out that with the modulator sensitivities that are available, the optical power can be increased to the point where net gain is realized.

The elucidation of the optical power dependency can also resolve one of the early debates in the development of analog links: given a diode laser, is it better to modulate it directly or to use this *same* laser as the CW source for an external modulator? The answer usually was that, of course, it is better to modulate directly, because the unavoidable loss of the modulator will always make external modulation have lower gain. However, as (2) and (3) show, this line of reasoning leads one away from a critical distinction. If the average optical power is low, external modulation will have lower gain, even if the modulator has no optical insertion loss. Conversely, if the CW optical power is high, then external modulation will yield higher gain than direct modulation, in spite of the additional modulator loss. This idea is best expressed by the crossover optical power $P_{I,\mathrm{cross}}$, which yields the same gain for direct and external modulation (2), (3)

$$P_{I,\mathrm{cross}} = \frac{2 V_\pi S_L}{t_{\mathrm{ff}} \pi \sqrt{R_{\mathrm{Las}} R_{\mathrm{Mod}}}}. \tag{4}$$

As can be seen in (4), $P_{I,\mathrm{cross}}$ is not a fixed number, but rather depends upon characteristics of the direct and external modulation-link devices—i.e., the semiconductor laser and the external modulator, respectively. These characteristics, particularly S_L and V_π, depend in turn upon the RF frequencies at which the devices were designed to operate, so $P_{I,\mathrm{cross}}$ is also frequency dependent to that extent. In [31], for instance, it was shown that direct and external modulation links at 50 MHz had the same gain for $P_{I,\mathrm{cross}} = 3$ mW. As manufacturers continue to improve device parameters, $P_{I,\mathrm{cross}}$ will vary accordingly. Equation (4) shows that $P_{I,\mathrm{cross}}$ at a given RF frequency will be decreased by improvements to the state of the art in modulator technology (i.e., lower V_π) and will be increased by improved lasers (i.e., lasers with larger S_L).

B. Link Noise Figure

NF is a critical parameter in antenna-remoting applications, but less so in distribution applications such as CATV. It can be expressed as

$$\mathrm{NF} = 10 \log \left[\frac{\overline{N_{\mathrm{out}}}}{kTg} \right] \tag{5}$$

where N_{out} is the total noise spectral density at the link output, k is Boltzmann's constant, and $T = 290°\mathrm{K}$. Thus, to obtain the effect of an individual noise source on the link NF, one divides the output noise due to that source by the link gain.

In any IMDD link the primary sources of noise are the photodetected optical intensity noise [usually dominated by laser relative intensity noise (RIN)], shot noise arising from the photodetection process, and thermal noise arising from the ohmic impedances of the RF source, modulation device, photodetector, and from ohmic losses in the interface circuitry between the source and modulation device and between the photodetector and the link output. The extent to which RIN, shot noise, and the various sources of thermal noise contribute to N_{out} are affected by the manner in which the modulation device and photodetector are impedance-matched to the link input and output impedances, respectively. However, only when the effects of RIN and shot noise are reduced to a level that is much lower than what has been achieved in most experimental IMDD links does thermal noise constitute a large portion of N_{out} [30].

For most direct modulation links, the laser RIN dominates over the laser shot noise and the thermal noises. The link output noise due to laser RIN can be expressed as

$$\bar{N}_{\mathrm{out,RIN}} = I_D^2 \cdot \mathrm{RIN} R_D \tag{6}$$

where RIN is the laser relative intensity noise at the analog-signal frequency and I_D is the average photocurrent. Equation (6) shows that noise caused by laser RIN increases as the square of average optical power. In (2), it was shown that direct modulation-link gain is independent of average optical power. Consequently, dividing a noise source which increases as the square of optical power by a gain which is independent of it yields an NF which increases as the square of optical power. The NF data in Fig. 4 for the FP laser (which had
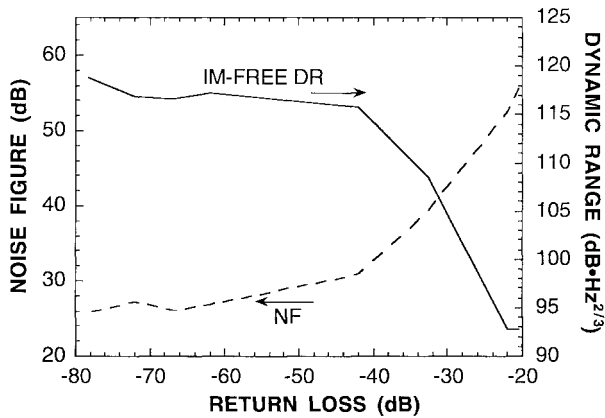
Fig. 5. NF and IM-free DR of a FP laser-based direct modulation link at 450 MHz as a function of backreflection to the commercially packaged laser.

Fig. 6. 450-MHz NF and IM-free DR of direct modulation links using commercial DFB versus commercial and repackaged FP lasers.

a RIN large enough to dominate the link NF) confirm this prediction.

State-of-the-art external modulation links often use a solid-state laser as the CW optical source. The relaxation frequency of these lasers is typically only a few hundred kilohertz. Recall that a laser's RIN spectrum falls off as f^{-2} above its relaxation frequency. Consequently, the RIN from these lasers has dropped to negligible levels by the time one reaches the lower passband frequency of most links. Therefore, the dominant output noise power-spectral density is due to detector shot noise, which can be expressed as

$$\bar{N}_{\text{out,shot}} = 2qI_D R_D. \tag{7}$$

To obtain the effects of shot noise on the NF, one again divides N_{out} by the link gain. Dividing a noise term which depends linearly on average optical power by a gain expression which depends quadratically on optical power yields an NF which *decreases* linearly with increasing optical power. Thus, despite the fact that increasing the link average optical power generates more shot-noise power at the link output, the effect of this increased shot noise is decreased at the link input because the link gain is increasing faster than the shot noise. This trend can be seen in the external modulation-link data in Fig. 4.

Fig. 4 also shows that the NF of DFB-based direct modulation links can be significantly lower than that of FP-based links. For lasers with the same slope efficiency, the difference in NF's can be traced to the lower RIN of the DFB as compared to the FP. The general impression is that lower RIN is due to the different laser *structure*, i.e., the DFB versus the FP. However, recent work of Roussell *et al.* [44] has demonstrated that control of optical reflections, especially in the laser packaging, is more important in reducing the RIN than the laser structure. Fig. 5 shows how the optical return loss of an FP semiconductor laser affects a typical direct modulation link's NF and IM-free DR (which is discussed further in greater detail in the following section). Fig. 6 compares the NF's of commercially-packaged FP and DFB diode lasers to FP lasers which were fiber-coupled in a way that minimized optical reflections back into the laser cavity. These data show that the FP laser can yield as low a link NF
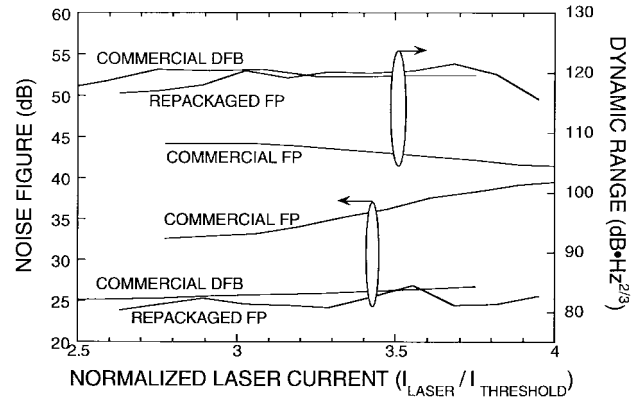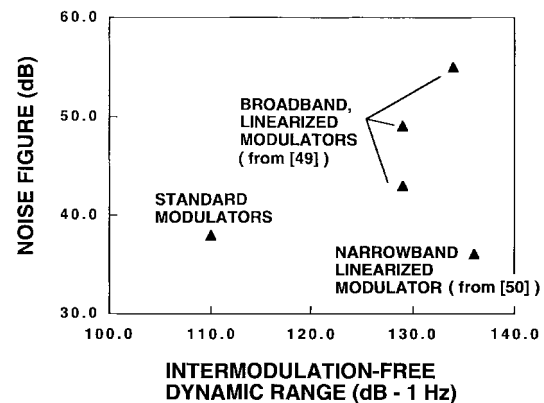

Fig. 7. Simulated NF versus IM-free DR of external modulation links using both standard and broad-band linearized modulators (after [49]).

as a DFB can. The NF's of FP lasers for direct modulation are quite consistent for a given device structure, but vary from 24 to 32 dB among different device structures and manufacturers [44].

Based on these results, the question may be raised as to whether or not we still need DFB's. The answer is "yes" for links with long fiber lengths. The deleterious effects of chromatic dispersion are smaller with the single-longitudinal-mode DFB than with the multimode FP. However, for shorter-length links where chromatic dispersion is negligible, these results suggest that if optical reflections (for example, from fiber connectors being repeatedly made and broken) can be controlled, appropriately packaged and fiber-coupled FP lasers may be adequate.

C. Link IM-Free Dynamic Range

The IM-free DR is an important parameter in links where multiple RF frequencies are simultaneously present. Thus, IM-free specifications are almost invariably seen in applications such as CATV distribution[2] and antenna receiving.

---

[2] The CATV industry determines distortion arising from the same underlying mechanisms by measuring the composite triple beat (CTB) and composite second order (CSO) produced when the link is fed by a multichannel signal generator whose number and spacing of channels matches the intended application.
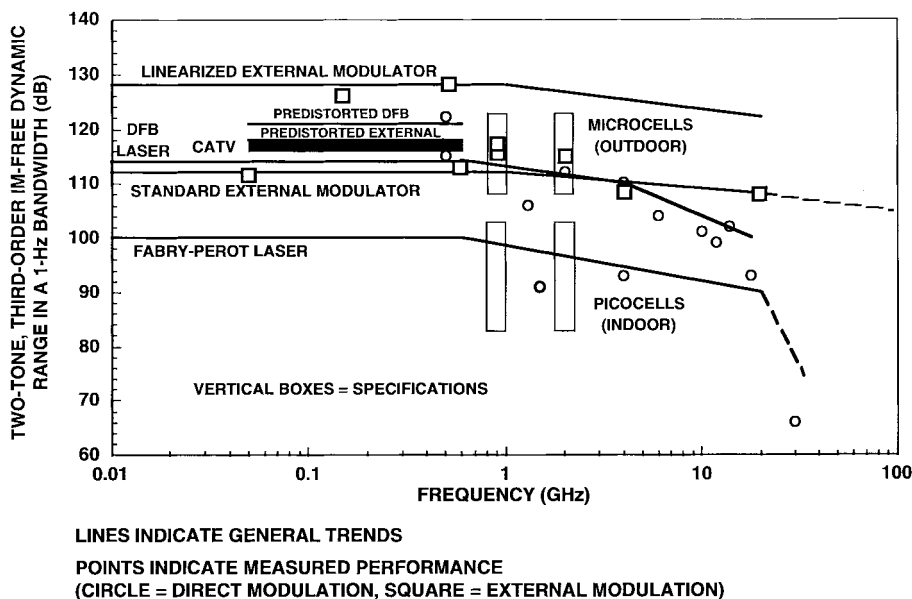
Fig. 8. Comparison of IM-free DR performance of several types of links: both standard (FP- and DFB-laser-based direct modulation, and MZI-based external modulation), and linearized (external modulation link with predistortion circuit, and a linearized external modulator-based link) to cellular telephony and CATV specifications.

The IM-free DR is defined as the maximum difference between the noise floor and the fundamental output which produces distortion terms of equal amplitude to the noise floor. The noise floor in turn depends on the link's instantaneous bandwidth (B), which varies by application. Consequently, to lend general applicability to the IM-free DR measurements, the results are often given in terms of a 1-Hz noise bandwidth. To use such results in a specific application simply requires scaling the 1-Hz data to the receiver's actual instantaneous bandwidth. The bandwidth scaling exponent depends on the order of the dominant distortion. Since many applications have an operational bandwidth less than an octave, the second-order distortion terms can be filtered out. Thus, for such applications, the lowest order in-band distortion is the third order, which causes the IM-free DR to scale as $B^{2/3}$.

Conventional wisdom has held that the IM-free DR of FP lasers is lower than that of DFB lasers—partially because the conventional view is that the FP's RIN is higher, and partially because in early DFB's the electrical isolation of the active region was used to achieve a more linear optical power versus laser-current curve. Representative IM-free DR measurements for commercially packaged FP and DFB lasers are shown in Fig. 6. The same techniques which improved the RIN, and hence, the NF of the FP can also improve their IM-free DR. Fig. 6 also shows IM-free DR data for a FP link using an optical isolator and a low-backreflection photodetector. As can be seen, this permits a FP to have approximately the same IM-free DR as the DFB [44].

The IM-free DR of an external modulation link is dominated by the type of external modulator and the average optical power. However, the IM-free DR for external modulation link using a standard MZ modulator is about the same as for a DFB-based direct modulation link.

Although in many links the distortion is dominated by the modulation device, in some links the photodetector or the fiber itself can contribute measurable distortion. Photodetector distortion usually does not become an issue with standard (i.e., unlinearized) modulation devices as discussed in Section II. Fiber-generated distortion can arise through the combined effects of modulation-device chirp, and fiber chromatic dispersion, and a large bandwidth × fiber length product. Since lithium–niobate MZI's have effectively zero chirp, fiber-generated distortion is generally not an issue in an external modulation link, where a kilohertz-linewidth solid-state laser can be used as the CW source.

For high-performance applications, among them CATV and radar antenna remoting, the required IM-free DR is 5–10 dB higher than the best results achieved for standard direct and external modulation links. The myriad techniques for extending the IM-free DR via linearization can be divided into two general categories: electro-optical (including predistortion, feedback, and feed-forward techniques, which will not be discussed further in this paper), and all-optical (such as the use of multielectrode modulators). There are a number of factors which enter into the selection of a linearization method. One key distinguishing feature is whether the linearization method is focused on reducing a particular order of distortion, such as the third, or whether the method reduces all distortion regardless of order.

Motivated largely by the CATV application, a number of all-optical linearization techniques which suppress both second- and third-order distortion have been developed [45]–[48]. These approaches are capable of significant improvement in DR, but at a cost of increased bias-control complexity; for example, up to four biases need to be controlled. Also, there is a tradeoff between linearization and the NF. This trend is made clear in Fig. 7, which plots the simulation results of Bridges and Schaffner [49] for several broad-band linearized modulator designs. For distribution applications, such as CATV, the NF is relatively unimportant, so this is a reasonable tradeoff to make.

In applications such as antenna remoting, the NF is a critical parameter, so its tradeoff with linearization can have severe consequences. However, as predicted analytically by Bridges and Schaffner [49] and confirmed experimentally by Betts [50], to linearize only the third order does not involve a NF penalty, as can be seen from the narrow-band data point in Fig. 7. Since virtually all antenna remoting links require only third-order linearization, these results suggest that it is not merely implementationally easier to use third-order-only linearization, but also technically important to do so.

Fig. 8 compares the IM-free DR performance of a linearized external modulator-based link to the performance of the three types of standard (not linearized) links discussed above. The IM-free DR of an external modulation link with a predistortion circuit is also shown, as are specifications for the performance of links for several commercial applications. For a more detailed comparison and discussion of all-optical linearization, the reader is referred to [49].

V. Summary

We have reviewed the state-of-the-art IMDD analog optical links. In doing so, we discussed advances in some of the most commonly used link components, including optical detectors, semiconductor laser diodes, and external modulators. Techniques for improving the NF and extending the DR performance of these links were also reviewed.

In addition to the technical trends discussed above, there is one overriding trend that has emerged as well. The initial applications of analog optical links were largely technology-driven ones where link performance was the primary requirement and the cost was secondary. These applications, while important for establishing the technology, have a limited market. We are now just seeing a much wider potential market in cost-driven applications, where cost is the primary factor, with perhaps a slight compromise in technical performance. The degree to which the field will be able to capitalize on this trend will be determined largely by its ability to reduce the cost of analog optical links without significantly reducing the technical performance.

Acknowledgment

The authors wish to thank F. O'Donnell, K. Ray, G. Rezendes, H. Roussell, M. Taylor, J. Vivilecchia, and A. Yee for assistance in obtaining some of the experimental link data reported. The views expressed in this paper are those of the authors and do not reflect the official policy or position of the U.S. Government.

References

[1] A. Seeds, "Optical transmission of microwaves," in *The Review of Radio Science*, W. Stone, Ed. London, U.K.: Oxford Univ. Press, 1996, pp. 325–360.
[2] P. Yu, "Optical receivers," in *Electronics Handbook*. Orlando, FL: CRC Press, 1996.
[3] C. Cox, V. Diaduk, I. Yao, F. Leonberger, and R. Williamson, "InP optoelectronic switches and their high-speed signal-processing applications," *Proc. SPIE–Int. Soc. Opt. Eng.*, vol. 439, pp. 164–168, 1983.
[4] A. Paollela, A. Madjar, and P. Herczfeld, "Modeling the GaAs MESFET's response to modulated light at radio and microwave frequencies," *IEEE Trans. Microwave Theory Tech.*, vol. 42, pp. 1122–1130, July 1992.
[5] R. Tucker, A. Taylor, C. Burrus, G. Eisenstein, and J. Wiesenfeld, "Coaxially mounted 67 GHz bandwidth InGaAs PIN photodiode," *Electron. Lett.*, vol. 22, pp. 917–918, 1986.
[6] J. Bowers and C. Burrus, "Heterojunction waveguide photodetectors," *Proc. SPIE–Int. Soc. Opt. Eng.*, vol. 716, pp. 109–113, 1987.
[7] ——, "Ultrawide-band long-wavelength p-i-n photodetectors," *IEEE J. Lightwave Technol.*, vol. LT-15, pp. 1339–1350, Oct. 1987.
[8] M. Makiuchi, H. Hamaguchi, T. Mikawa, and O. Wada, "Easily manufactured high-speed back-illuminated GaInAs/InP p-i-n photodiode," *IEEE Photon. Technol. Lett.*, vol. 3, pp. 530–531, June 1991.
[9] E. Ozbay, K. Li, and D. Bloom, "2.0-ps 150-GHz GaAs monolithic photodiode and all-electronic sampler," *IEEE Photon. Technol. Lett.*, vol. 3, pp. 570–572, June 1991.
[10] Y. Chen, S. Williamson, T. Brock, F. Smith, and A. Calawa, "375 GHz bandwidth photoconductive detector," *Appl. Phys. Lett.*, vol. 59, pp. 1984–1986, 1991.
[11] D. Wake, T. Spooner, S. Perrin, and I. Henning, "50 GHz InGaAs edge-coupled pin photodetector," *Electron. Lett.*, vol. 27, pp. 1073–1075, 1991.
[12] K. Kato, S. Hata, A. Kozen, J. Yoshida, and K. Kawano, "Highly efficient 40-GHz waveguide InGaAs p-i-n photodiode employing multimode waveguide structure," *IEEE Photon. Technol. Lett.*, vol. 3, pp. 820–822, Sept. 1991.
[13] Y. Wey, K. Giboney, J. Bowers, M. Rodwell, P. Silvestre, P. Thiagarajan, and G. Robinson, "108-GHz GaInAs/InP p-i-n photodiodes with integrated bias tees and matched resistors," *IEEE Photon. Technol. Lett.*, vol. 5, pp. 1310–1312, Nov. 1993.
[14] K. Kato, A. Kozen, Y. Maramoto, T. Nagatsuma, and M. Yaita, "110-GHz, 50%-efficiency mushroom-mesa waveguide p-i-n photodiode for a 1.55-μm wavelength," *IEEE Photon. Technol. Lett.*, vol. 6, pp. 719–721, June 1994.
[15] K. Giboney, J. Bowers, and M. Rodwell, "Travelling-wave photodetectors," in *IEEE Microwave Theory Tech. Symp. Dig.*, Orlando, FL, May 1995, pp. 159–162.
[16] W. Way, "Large signal nonlinear distortion prediction for a single-mode laser diode under microwave intensity modulation," *J. Lightwave Technol.*, vol. LT-5, pp. 305–315, Mar. 1987.
[17] K. Williams, R. Esman, and M. Dagenais, "Nonlinearities in p-i-n microwave photodetectors," *IEEE Photon. Technol. Lett.*, vol. 14, pp. 94–96, Jan. 1996.
[18] G. A. Davis, R. E. Weiss, R. A. LaRue, K. J. Williams, and R. D. Esman, "A 920–1650-nm high-current photodetector," *IEEE Photon. Technol. Lett.*, vol. 14, pp. 94–96, Oct. 1996.
[19] L. Lin, M. Wu, T. Itoh, T. Vang, R. Muller, D. Sivco, and A. Cho, "Velocity-matched distributed photodetectors with high saturation power and large bandwidth," *IEEE Photon. Technol. Lett.*, vol. 8, pp. 1376–1378, Oct. 1996.
[20] E. Ackerman, D. Kasemset, S. Wanuga, D. Hogue, and J. Komiak, "A high-gain directly modulated *L*-band microwave optical link," in *IEEE Microwave Theory Tech. Symp. Dig.*, Dallas, TX, May 1990, pp. 153–155.
[21] C. Cox, D. Tsang, L. Johnson, and G. Betts, "Low-loss analog fiber-optic links," in *IEEE Microwave Theory Tech. Symp. Dig.*, Dalls, TX, May 1990, pp. 157–160.
[22] C. Cox, "Intrinsic gain in analog fiber-optic links and its effect on noise figure," presented at the *XXIV Gen. Assembly, Int. Union Radio Sci.*, Kyoto, Japan, Aug. 1993.
[23] E. Ackerman, D. Kasemset, S. Wanuga, R. Boudreau, J. Schlafer, and R. Lauer, "A low-loss Ku-band directly modulated fiber optic link," *IEEE Photon. Technol. Lett.*, vol. 3, pp. 185–187, Feb. 1991.
[24] D. Atlas, "A 20-GHz bandwidth InGaAsP/InP MTBH laser module," *IEEE Photon. Technol. Lett.*, vol. 5, pp. 123–212, Feb. 1993.
[25] D. Davies and A. Goutzoulis, "Wavelength-multiplexed analog fiber optic link for wideband radio-frequency and local oscillator signal transmission," *Opt. Eng.*, vol. 31, pp. 2323–2329, 1992.
[26] H. Wang and M. Wechsberg, private communication, 1996.
[27] K. Vahala, M. Newkirk, and T. Chen, "The optical gain lever: A novel gain mechanism in the direct modulation of quantum well semiconductor lasers," *Appl. Phys. Lett.*, vol. 54, pp. 2506–2508, 1989.
[28] J. Ralston, S. Weisser, K. Eisele, R. Sah, E. Larkins, J. Rosenzweig, J. Fleissner, and K. Bender, "Low-bias-current direct modulation up to 33 GHz in InGaAs/GaAs/AlGaAs pseudomorphic MQW ridge-waveguide devices," *IEEE Photon. Technol. Lett.*, vol. 6, pp. 1076–1079, Sept. 1994.

[29] K. Lau, "Narrow-band modulation of semiconductor lasers at millimeter wave frequencies (>100 GHz) by mode locking," *IEEE J. Quantum Electron.*, vol. 26, pp. 250–261, Feb. 1990.

[30] C. Cox, E. Ackerman, and G. Betts, "Relationship between gain and noise figure of an optical analog link," in *IEEE Microwave Theory Tech. Symp. Dig.*, San Francisco, CA, June 1996, pp. 1551–1154.

[31] C. Cox, G. Betts, and L. Johnson, "An analytic and experimental comparison of direct and external modulation in analog fiber-optic links," *IEEE Trans. Microwave Theory Tech.*, vol. 38, pp. 501–509, May 1990.

[32] E. Ackerman, D. Kasemset, and S. Wanuga, "An external modulation L-band link with 117 dB spurious-free dynamic range," *Microwave J.*, vol. 34, pp. 158–164, 1991.

[33] C. Cox *et al.*, "Incrementally lossless, broad-bandwidth analog fiber-optic link," in *Proc. IEEE LEOS Summer Meeting (LEOS-STM'90)*, Monterrey, CA, July 1990, pp. 15–16.

[34] S. Merritt, W. Glomb, and J. Farina, "Minimum noise figure microwave transmission system," presented at the *2nd. Annu. DARPA/Rome Laboratory Symp.*, Monterrey, CA, Dec. 1991.

[35] G. Betts, C. Cox, and K. Ray, "20-GHz optical analog link using an external modulator," *IEEE Photon. Technol. Lett.*, vol. 2, pp. 923–925, Dec. 1990.

[36] S. Pappert, M. Berry, S. Hart, R. Orazi, and S. Li, "Remote multioctave electromagnetic field measurements using analog fiber optic links," presented at the *IEEE Antennas Propagat. Soc. Int. Symp.*, Chicago, IL, 1992.

[37] K. Noguchi *et al.*, "Low-voltage and broad-band Ti:LiNbO$_3$ modulator operating in the millimeter wavelength region," in *OFC'96*, San Franciso, CA, Jan. 1996, pp. 205–206.

[38] W. Bridges and F. Sheehy, "Velocity-matched electro-optic modulator," in *Proc. SPIE*, vol. 1371, San Jose, CA, Sept. 1990, pp. 68–77..

[39] R. Welstand, C. Sun, S. Pappert, Y. Liu, J. Chen, J. Zhu, A. Kellner, and P. Yu, "Enhanced dynamic range property of Franz–Keldysh effect waveguide modulator," *IEEE Photon. Technol. Lett.*, vol. 7, pp. 751–753, July 1995.

[40] C. Sun, S. Pappert, R. Welstand, T. Zhu, P. Yu, Y. Liu, and J. Chen, "High spurious-free dynamic range fiber link using a semiconductor electroabsorption modulator," *Electron. Lett.*, vol. 31, pp. 902–903, May 1995.

[41] R. Walker, "High-speed III–V semiconductor intensity modulators," *IEEE J. Quantum Electron.*, vol. 27, pp. 654–667, Mar. 1991.

[42] W. Wang, D. Chen, H. Fetterman, Y. Shi, W. Steier, L. Dalton, and P. Chow, "Optical heterodyne detection of 60 GHz electrooptic modulation from polymer waveguide modulators," *Appl. Phys. Lett.*, vol. 67, pp. 1806–1808, 1995.

[43] C. H. Cox, "Gain and noise figure in analogue fiber-optic links," *Proc. Inst. Elect. Eng.*, vol. 139, pt. J, pp. 238–242, 1992.

[44] H. Roussell, R. Helkey, G. Betts, and C. Cox, "Effect of optical feedback on high dynamic range Fabry–Perot laser optical links," *IEEE Photon. Technol. Lett.*, vol. 9, pp. 106–108, Jan. 1997..

[45] S. Korotky and R. DeRidder, "Dual parallel modulation schemes for low-distortion analog optical transmission," *IEEE J. Select. Areas Commun.*, vol. 8, pp. 1377–1381, Sept. 1990.

[46] P. Liu, B. Li, and Y. Tirson, "In search of a linear electrooptic amplitude modulator," *IEEE Photon. Technol. Lett.*, vol. 3, pp. 144–146, Feb. 1991.

[47] M. Farwell, Z. Lin, E. Wooten, and W. Chang, "An electrooptic intensity modulator with improved linearity," *IEEE Photon. Technol. Lett.*, vol. 3, pp. 792–795, Sept. 1991.

[48] H. Skeie and R. Johnson, "Linearization of electro-optic modulators by a cascade coupling of phase modulating electrodes," *Proc. SPIE–Int. Soc. Opt. Eng.*, vol. 1583, pp. 153–163, 1991.

[49] W. Bridges and J. Schaffner, "Distortion in linearized electro-optic modulators," *J. Lightwave Technol.*, vol. 43, pp. 2184–2197, Sept. 1995.

[50] G. Betts, "Linearized modulator for suboctave-bandpass optical analog links," *IEEE Trans. Microwave Theory Tech.*, vol. 42, pp. 2642–2649, Dec. 1994.

Charles Cox (S'78–M'78–SM'95) received the B.S.E.E. and M.S.E.E. degrees from the University of Pennsylvania, Philadelphia, PA, in 1970 and 1972, respectively, and the Sc.D. degree from the Massachusetts Institute of Technology (MIT) Lexington, MA, in 1979.

Since 1979, he has been with MIT Lincoln Laboratory, where he has been a Technical Staff Member in the Photovoltaic Systems and the Applied Photonics Groups. He is presently a Senior Staff Member in the applied photonics section of the Radar Systems Group. For the last 12 years, he has both theoretically and experimentally pursued the development of electo-optic devices and analog fiber optic links, primarily for antenna remoting.

Dr. Cox is a member of the Optical Society of America and Sigma Xi.

Edward I. Ackerman (S'76–M'87) received the B.S. degree in electrical engineering from Lafayette College, Easton, PA, in 1987, and the M.S. and Ph.D. degrees in electrical engineering from Drexel University, Philadelphia, PA, in 1989 and 1994, respectively.

From 1989 to 1994, he was employed as a Microwave Photonics Engineer at Martin Marietta's Electronics Laboratory in Syracuse, NY. He is currently a Technical Staff Member at the Massachusetts Institute of Technology (MIT) Lincoln Laboratory, Lexington, where he develops high-performance analog photonic links for microwave communications and antenna remoting applications.

Roger Helkey (M'88) received the B.S. degree in engineering (with honors) from the California Institute of Technology, Pasadena, in 1982, and the M.S. and Ph.D. degrees in electrical engineering from the University of California at Santa Barbara, in 1993.

From 1993 to 1995, he was a Researcher at both the University of Tokyo, and Advanced Telecommunications Research, Japan, where he studied microcavity effects and nonlinear optical switching. From 1982 to 1984, he was a Design Engineer at Trimble Navigation, where he was responsible for the design of digital and analog circuits in the development of a global positioning system (GPS) receiver. From 1984 to 1986, he was a Technical Staff Member at Watkins-Johnson, where he was responsible for microwave component and subsystem design. He is currently a Staff Member with the Massachusetts Institute of Technology (MIT) Lincoln Laboratory, Lexington, MA, where he is working on high-performance analog optical links. He is a co-author of a book chapter and holds several patents.

Gary E. Betts (S'84–M'84), for a photograph and biography, see this issue, p. 1287.